Charged lepton flavor violation in supersymmetry with bilinear *R*-parity violation

D. F. Carvalho,* M. E. Gómez,† and J. C. Romão‡
Departamento de Física, Instituto Superior Técnico, Av. Rovisco Pais 1, 1049-001 Lisboa, Portugal
(Received 19 February 2002; published 14 May 2002)

The simplest unified extension of the minimal supersymmetric standard model with bilinear *R*-parity violation naturally predicts a hierarchical neutrino mass spectrum, suitable to explain atmospheric and solar neutrino fluxes. We study whether the individual violation of the lepton numbers $L_{e,\mu,\tau}$ in the charged sector can lead to measurable rates for BR($\mu\to e\gamma$) and BR($\tau\to\mu\gamma$). We find that some of the *R*-parity violating terms that are compatible with the observed atmospheric neutrino oscillations could lead to rates for $\mu\to e\gamma$ measurable in projected experiments. However, the Δm^2_{12} obtained for those parameters is too high to be compatible with the solar neutrino data, excluding therefore the possibility of having measurable rates for $\mu\to e\gamma$ in the model.

DOI: 10.1103/PhysRevD.65.093013 PACS number(s): 14.60.Pq, 12.60.Jv

I. INTRODUCTION

In the standard model (SM), lepton number is exactly preserved in contradiction with the observed neutrino oscillations [1,2]. Several extensions of the SM include patterns of neutrino masses and mixings which can provide a satisfactory explanation for these flavor oscillations. The consequences of the individual violation of the lepton numbers $L_{e,\mu,\tau}$ for charged leptons will be manifest in processes such as $\mu\to e\gamma$, $\mu\to 3e$, μ-e conversion in heavy nuclei, $\tau\to\mu\gamma$ and $K_L\to\mu e$ [3]. The experimental upper bound for these processes is quite restrictive, which imposes a significant constraint for the explanation of flavor in models beyond the SM. However, the mechanisms used to explain the origin of the tiny neutrino masses required to explain solar and atmospheric neutrino oscillations typically imply that these processes may occur at small rates, motivating an increasing experimental interest in exploring further charged lepton flavor violating processes.

The rates for charged lepton flavor violation (LFV) are extremely small in the SM with right-handed neutrinos ($\propto\Delta m_\nu^4/M_W^4$ [4]). In *R*-parity conserving supersymmetric (SUSY) models, such as the minimal supersymmetric standard model (MSSM), the presence of LFV processes is associated with vertices involving leptons and their superpartners [5]. These processes are sensitive to the scalar mass matrices structure, a nondiagonality of the latter in a basis in which fermions are diagonal leads to a hard violation of flavor. The structure of the scalar mass matrices is very sensitive to the SUSY breaking; in particular in models where SUSY is softly broken, LFV imposes a severe constraint in the flavor dependence of the soft terms as they are generated in grand unified theories (GUT's) and string inspired models [6].

The inclusion of a ''seesaw'' mechanism in the MSSM provides a very attractive scenario to understand neutrino oscillations with very small neutrino masses, and at the same time gives rates for LFV processes accessible in projected experiments [7,8]. The waiving of the *R*-parity symmetry in the MSSM provides an alternative scenario to explain the generation of small neutrino masses. In this case the *R*-parity violating operators can be constrained by rare processes [9–12].

The simplest extension of the MSSM with bilinear *R*-parity violation (BRPV) [13,14] (allowing *B*-conserving but *L*-violating interactions) can explain neutrino masses and mixings which can account for the observed neutrino oscillations [15]. The BRPV model has been extensively discussed in the literature [16]. It is motivated by the fact that it provides an effective truncation of models where *R* parity breaks *spontaneously* by singlet sneutrino vacuum expectation values (VEV's) around the weak scale [17]. Moreover, it allows for the radiative breaking of *R* parity, opening also new ways to unify gauge and Yukawa couplings [18] and with a potentially slightly lower prediction for α_s [19]. For recent papers on phenomenological implications of these models see Refs. [20,21]. As the parameters involved in the *R*-parity violating operator are constrained in order to predict neutrino masses in the sub-eV range, we address in this paper the question of whether this operator will induce rates for charged LFV processes of experimental interest. Some of them occur at tree level such as double β decay [12,22] and μ-e conversion in nuclei [23]. One loop LFV decays as $l_j\to l_i\gamma$ become interesting in this framework due to the experimental interest in improving the current limits [24]:

$$\mathrm{BR}(\mu\to e\gamma)<1.2\times10^{-11},$$

$$\mathrm{BR}(\tau\to\mu\gamma)<1.1\times10^{-6},$$

$$\mathrm{BR}(\tau\to e\gamma)<2.7\times10^{-6}. \quad (1)$$

As we will show, the predictions for the last two processes are much lower than the above limits and will not constrain the BRPV model. For $\mu\to e\gamma$ the predictions are compatible with the current limit but could begin to constrain the model for the bounds that will be reached in current [25] or planned experiments [26], if only the atmospheric neutrino data are taken in account. However the requirement that the one-loop induced Δm^2_{12} is in agreement with the solar neutrino data

*Electronic address: dani@cfif.ist.utl.pt
†Electronic address: mgomez@cfif.ist.utl.pt
‡Electronic address: jorge.romao@ist.utl.pt

implies that the predicted rates for $\mu \to e\gamma$ will not be visible, even in those new experiments.

This paper is organized as follows. In Secs. II, III and IV we describe the model, the scalar potential and the fermion mass matrices, respectively. In Sec. V we derive the expressions for the LFV processes. The results are presented in Sec. VI and in Sec. VII we give our conclusions. The more technical questions regarding the mass matrices, couplings and the explicit formulas for the amplitudes are given in the Appendixes.

II. THE SUPERPOTENTIAL AND THE SOFT BREAKING TERMS

Using the conventions of Refs. [21,27] we introduce the model by specifying the superpotential, which includes BRPV [16] in three generations. It is given by

$$W = \varepsilon_{ab}[h_U^{ij}\hat{Q}_i^a\hat{U}_j\hat{H}_u^b + h_D^{ij}\hat{Q}_i^b\hat{D}_j\hat{H}_d^a + h_E^{ij}\hat{L}_i^b\hat{R}_j\hat{H}_d^a - \mu\hat{H}_d^a\hat{H}_u^b + \epsilon_i\hat{L}_i^a\hat{H}_u^b] \tag{2}$$

where the couplings h_U, h_D and h_E are 3×3 Yukawa matrices and μ and ϵ_i are parameters with units of mass. The second bilinear term in Eq. (2) violates lepton number and therefore also breaks R parity. The inclusion of the R-parity violating term, although small, can modify the predictions of the MSSM. The most salient features are that neutrinos become massive and the lightest neutralino is no longer a dark matter candidate because it is allowed to decay. Furthermore, we can observe that this model implies the mixing of the leptons with the usual charginos and neutralinos of the MSSM. Lepton Yukawa couplings can be written as diagonal matrices without any loss of generality since it is possible to rotate the superfields $\hat{L}_i^b$ in the superpotential, Eq. (2), such that Yukawa matrix h_E becomes diagonal. Conversely, in BRPV models it is possible to apply a similar rotation to reduce the number of ϵ parameters and provide a nontrivial structure to h_E [28].

Supersymmetry breaking is parametrized with a set of soft supersymmetry breaking terms. In the MSSM these are given by

$$\mathcal{L}_{\text{soft}} = -V_{\text{soft}}^{\text{MSSM}} + \left[\frac{1}{2}M_s\lambda_s\lambda_s + \frac{1}{2}M\lambda\lambda + \frac{1}{2}M'\lambda'\lambda' + \text{H.c.}\right] \tag{3}$$

where

$$\begin{aligned} V_{\text{soft}}^{\text{MSSM}} = {} & M_Q^{ij2}\tilde{Q}_i^{a*}\tilde{Q}_j^a + M_U^{ij2}\tilde{U}_i\tilde{U}_j^* + M_D^{ij2}\tilde{D}_i\tilde{D}_j^* + M_L^{ij2}\tilde{L}_i^{a*}\tilde{L}_j^a \\ & + M_R^{ij2}\tilde{R}_i\tilde{R}_j^* + m_{H_d}^2H_d^{a*}H_d^a + m_{H_u}^2H_u^{a*}H_u^a \\ & + \varepsilon_{ab}[A_U^{ij}\tilde{Q}_i^a\tilde{U}_jH_u^b + A_D^{ij}\tilde{Q}_i^b\tilde{D}_jH_d^a + A_E^{ij}\tilde{L}_i^b\tilde{R}_jH_d^a \\ & - B\mu H_d^aH_u^b]. \end{aligned} \tag{4}$$

In addition to the MSSM soft SUSY breaking terms in $V_{\text{soft}}^{\text{MSSM}}$ the BRPV model contains the following extra term:

$$V_{\text{soft}}^{\text{BRPV}} = -B_i\epsilon_i\varepsilon_{ab}\tilde{L}_i^aH_u^b, \tag{5}$$

where the B_i have units of mass.

The electroweak symmetry is broken when the two Higgs doublets H_d and H_u and the neutral component of the slepton doublets $\tilde{L}_i$ acquire vacuum expectation values. We introduce the notation:

$$H_d = \begin{pmatrix} H_d^0 \\ H_d^- \end{pmatrix}, \quad H_u = \begin{pmatrix} H_u^+ \\ H_u^0 \end{pmatrix}, \quad \tilde{L}_i = \begin{pmatrix} \tilde{L}_i^0 \\ \tilde{l}_i^- \end{pmatrix}, \tag{6}$$

where we shift the neutral fields with nonzero VEV's as

$$H_d^0 \equiv \frac{\sigma_d^0 + v_d + i\varphi_d^0}{\sqrt{2}}, \quad H_u^0 \equiv \frac{\sigma_u^0 + v_u + i\varphi_u^0}{\sqrt{2}},$$

$$\tilde{L}_i^0 \equiv \frac{\tilde{\nu}_i^R + v_i + i\tilde{\nu}_i^I}{\sqrt{2}}. \tag{7}$$

Note that the W boson acquires a mass $m_W^2 = \frac{1}{4}g^2v^2$, where $v^2 \equiv v_d^2 + v_u^2 + v_1^2 + v_2^2 + v_3^2 \simeq (246\ \text{GeV})^2$.

In addition to the above MSSM parameters, our model contains nine new parameters, ϵ_i, v_i and B_i. The minimization of the scalar potential allows us to relate some of these free parameters. The values of ϵ_i, v_i are directly related to the neutrino masses and mixings as we will discuss below.

III. THE SCALAR POTENTIAL

The electroweak symmetry is broken when the neutral Higgs bosons and the neutral slepton fields acquire nonzero VEV's. These are calculated via the minimization of the effective potential or, in the diagrammatic method, via the tadpole equations. The full scalar potential at tree level is

$$V_{total}^0 = \sum_i \left|\frac{\partial W}{\partial z_i}\right|^2 + V_D + V_{\text{soft}}^{\text{MSSM}} + V_{\text{soft}}^{\text{BRPV}} \tag{8}$$

where z_i is any one of the scalar components of the superfields in the superpotential in Eq. (2), V_D are the D terms, and $V_{\text{soft}}^{\text{BRPV}}$ is given in Eq. (5).

The tree level scalar potential contains the following linear terms:

$$V_{linear}^0 = t_d^0\sigma_d^0 + t_u^0\sigma_u^0 + t_1^0\tilde{\nu}_1^R + t_2^0\tilde{\nu}_2^R + t_3^0\tilde{\nu}_3^R, \tag{9}$$

where the different t^0 are the tadpoles at tree level; their explicit expressions can be found in Ref. [15]. The five tree level tadpoles t_α^0 are equal to zero at the minimum of the tree level potential, and therefore we can use them to express the parameters

$$\mu, B, B_1, B_2, B_3 \tag{10}$$

in terms of

$$v_u, v_d, \epsilon_i, v_i, M_{Lij}^2, m_{H_u}^2, m_{H_d}^2. \tag{11}$$

We have two possible solutions for μ:

$$\mu = \frac{-b \pm \sqrt{b^2 - 4ac}}{2a} \tag{12}$$

where $a = v_u^2 - v_d^2$, $b = 2v_d \Sigma_{i=1}^3 \epsilon_i v_i$, and

$$c = v_u^2 \left(\sum_{i=1}^3 \epsilon_i^2 + m_{H_u}^2 \right) - v_d^2 m_{H_d}^2 - \left(\sum_{i=1}^3 \epsilon_i v_i \right)^2 - Dv^2 - \frac{1}{2} \sum_{i=1}^3 \sum_{j=1}^3 v_i v_j (M_{Lij}^2 + M_{Lji}^2), \tag{13}$$

where we have defined $D = \frac{1}{8}(g^2 + g'^2)(v_1^2 + v_2^2 + v_3^2 + v_d^2 - v_u^2)$.

As one can easily verify, the above relations lead to the MSSM relation for μ^2 in the limit of vanishing ϵ_i and v_i. The uncertainty of the sign in the MSSM is translated here into two possible values for the μ term. However for the values of ϵ_i and v_i relevant to our work both solutions are close in modulus and of opposite sign. The values for B and B_i can be expressed in terms of μ as

$$B = \frac{1}{v_u} \left[\frac{v_d}{\mu} (m_{H_d}^2 + \mu^2 + D) - \sum_{i=1}^3 \epsilon_i v_i \right], \tag{14}$$

$$B_i = \frac{1}{v_u} \left[v_d \mu - \sum_{j=1}^3 \epsilon_j v_j - \frac{1}{\epsilon_i} \left(Dv_i + \frac{1}{2} \sum_{j=1}^3 v_j (M_{Lij}^2 + M_{Lji}^2) \right) \right]. \tag{15}$$

The equivalent equations for the MSSM equations are obtained by setting ϵ_i, v_i equal to zero.

IV. FERMION MASSES WITH BRPV

As we discussed in the previous section the presence of BRPV terms in the superpotential, Eq. (2), induces nonzero VEV's for the sneutrinos and enables the neutrinos to have a mass, with a value related to the size of ϵ_i, v_i and the SUSY parameters involved in the electroweak symmetry breaking. Furthermore, the nonconservation of the R parity allows the SUSY partners to mix with the SM particles. In this section we describe in detail the resulting neutralino-neutrino and chargino-charged-lepton mass matrices, since they are the most directly related to our problem. The complete set of mass matrices for the BRPV model can be found in Ref. [15].

A. Neutralino-neutrino mass matrix

The range of values of the ϵ parameters is indirectly associated with the size of the neutrino masses predicted by the model. To explore this relation we describe next the mass mixings among neutralinos and neutrinos. In the basis $\psi^{0T} = (-i\lambda', -i\lambda^3, \tilde{H}_d^0, \tilde{H}_u^0, \nu_e, \nu_\mu, \nu_\tau)$ the neutral fermion mass matrix $\boldsymbol{M}_N$ is given by

$$\boldsymbol{M}_N = \begin{bmatrix} \mathcal{M}_{\chi^0} & m^T \\ m & 0 \end{bmatrix} \tag{16}$$

where

$$\mathcal{M}_{\chi^0} = \begin{bmatrix} M_1 & 0 & -\frac{1}{2}g' v_d & \frac{1}{2}g' v_u \\ 0 & M_2 & \frac{1}{2}g v_d & -\frac{1}{2}g v_u \\ -\frac{1}{2}g' v_d & \frac{1}{2}g v_d & 0 & -\mu \\ \frac{1}{2}g' v_u & -\frac{1}{2}g v_u & -\mu & 0 \end{bmatrix} \tag{17}$$

is the standard MSSM neutralino mass matrix and

$$m = \begin{bmatrix} -\frac{1}{2}g' v_1 & \frac{1}{2}g v_1 & 0 & \epsilon_1 \\ -\frac{1}{2}g' v_2 & \frac{1}{2}g v_2 & 0 & \epsilon_2 \\ -\frac{1}{2}g' v_3 & \frac{1}{2}g v_3 & 0 & \epsilon_3 \end{bmatrix} \tag{18}$$

characterizes the breaking of R parity.

The mass matrix $\boldsymbol{M}_N$ is diagonalized by

$$\mathcal{N}^* \boldsymbol{M}_N \mathcal{N}^{-1} = \mathrm{diag}(m_{\chi_i^0}, m_{\nu_j}), \tag{19}$$

where $(i = 1, \ldots, 4)$ for the neutralinos, and $(j = 1, \ldots, 3)$ for the neutrinos.

Since $m_\nu \ll m_{\chi^0}$ the mass matrix $\boldsymbol{M}_N$ is similar to the "see-saw" mass matrices and takes approximately the form $\mathrm{diag}(\mathcal{M}_{\chi^0}, m_{eff})$, with

$$m_{eff} = -m\, \mathcal{M}_{\chi^0}^{-1} m^T = \frac{M_1 g^2 + M_2 g'^2}{4 \det(\mathcal{M}_{\chi^0})} \begin{pmatrix} \Lambda_e^2 & \Lambda_e \Lambda_\mu & \Lambda_e \Lambda_\tau \\ \Lambda_e \Lambda_\mu & \Lambda_\mu^2 & \Lambda_\mu \Lambda_\tau \\ \Lambda_e \Lambda_\tau & \Lambda_\mu \Lambda_\tau & \Lambda_\tau^2 \end{pmatrix}, \tag{20}$$

where the Λ_i parameters in Eq. (20) are defined as

$$\Lambda_i \equiv \mu v_i + v_d \epsilon_i. \tag{21}$$

One of the neutrino species acquire a tree level nonzero mass, given by

$$m_{\nu_3} = \mathrm{Tr}(m_{eff}) = \frac{M_1 g^2 + M_2 g'^2}{4 \det(\mathcal{M}_{\chi^0})} |\vec{\Lambda}|^2, \tag{22}$$

where $|\vec{\Lambda}|^2 \equiv \Sigma_{i=1}^3 \Lambda_i^2$. The two other neutrinos can get masses at one loop as discussed in Refs. [15,29,30]. For our purposes it will be important to have an estimate of the val-

ues of $\Delta m_{12}^2 = m_{\nu_2}^2 - m_{\nu_1}^2$. We will use the results of Ref. [31] where it was found that, to a very good approximation, $m_{\nu_1} = 0$ and

$$m_{\nu_2} = \frac{3}{16\pi^2} m_b \sin 2\theta_b \frac{h_b^2}{\mu^2} \log \frac{m_{\tilde{b}_2}^2}{m_{\tilde{b}_1}^2} \frac{(\vec{\epsilon}\times\vec{\Lambda})^2}{|\vec{\Lambda}|^2}. \quad (23)$$

The explanation of the data on neutrino oscillations given in Ref. [15] requires the neutrino masses to be in the sub-eV range in order to fit the data on atmospheric neutrino oscillations. In our examples we take $m_{\nu_3} = 0.1$ eV, which leads to values of $|\vec{\Lambda}|$ in the range of 0.1–1 GeV^2, for the values of the SUSY parameters that we will consider. Considering that we take positive values for μ we should also take negative values for the product $\epsilon_i v_i$ to avoid our analysis being constrained to small values of ϵ_i. However, as we will see, for the values of the SUSY parameters that give the largest BR($\mu \to e\gamma$), the values of $|\epsilon_i|$ have to be below 0.1 GeV, if $\Delta m_{12}^2 < 10^{-4}$ (eV)^2, as required by the solar neutrino data.

B. Chargino–charged-lepton mass matrix

Due to the *R*-parity violating terms in the superpotential, Eq. (2), the charginos mix with the charged leptons, linking therefore the problem of the masses of the neutrinos with the problem of charged lepton flavor violation. We describe in this subsection the chargino-lepton mass matrix to explain how the flavor mixing on the charged lepton sector arises. In a basis where

$$\psi^{+T} = (-i\lambda^+, \tilde{H}_u^+, e_R^+, \mu_R^+, \tau_R^+),$$

$$\psi^{-T} = (-i\lambda^-, \tilde{H}_d^-, e_L^-, \mu_L^-, \tau_L^-), \quad (24)$$

the corresponding charged fermion mass terms in the Lagrangian are

$$\mathcal{L}_m = -\frac{1}{2}(\psi^{+T}, \psi^{-T}) \begin{pmatrix} 0 & M_C^T \\ M_C & 0 \end{pmatrix} \begin{pmatrix} \psi^+ \\ \psi^- \end{pmatrix} + \text{H.c.} \quad (25)$$

where the chargino–charged-lepton mass matrix M_C is given in Appendix A. As in the MSSM, M_C is diagonalized by two rotation matrices, and we include the physical charged leptons and charginos into a set of five charged fermions defined as

$$F_i^- = U_{ij}\psi_j^-, \quad F_i^+ = V_{ij}\psi_j^+, \quad (26)$$

such that

$$\boldsymbol{U^* M_C V^{-1} = M_{CD}} \quad (27)$$

where $\boldsymbol{M_{CD}}$ is the diagonal charged fermion mass matrix.

In the previous expressions the $F_i^\pm$ are two component spinors. We construct the four component Dirac spinors out of the two component spinors with the conventions (here we depart from the conventions of Ref. [27] because we want the e^-, μ^- and τ^- to be the particles and not the antiparticles)

$$\chi_i^- = \begin{pmatrix} F_i^- \\ F_i^+ \end{pmatrix}. \quad (28)$$

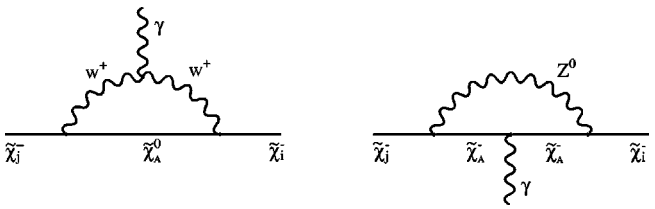

FIG. 1. Generic Feynman diagrams for $A_{L,Rij}^G$.

The parametrization of the matrices V and U given in Appendix A, which was introduced in Refs. [22,32], provides a very accurate representation of the exact result. By comparing the numerical results with the analytical expressions shown in Appendix A, we found discrepancies of less than 1%. To obtain this level of accuracy we had to introduce corrections in the definitions of V_L, V_R, and Ω_R with respect to the formulas of Ref. [22]. These arise mainly from including the submatrix E' in our derivation (see Appendix A). Although the matrix elements of E' are smaller than the other components of M_C, it must be taken into account in order to match the results of the smaller elements of U and V found in the exact diagonalization. Our definition of V_L and V_R leads to the correct form for the lower right 3×3 submatrices of U and V. We will make use of it to explain the details of our results. The inclusion of the matrix E' in the determination of Ω_R allows us to display the dependence of the matrix elements on the Λ parameters, rather than the explicit dependence on the ϵ's as quoted in Ref. [22].

Also, we must observe that the elements of Ω_L exceed the ones of Ω_R by several orders of magnitude. Therefore we can anticipate that the couplings containing the matrix V in Appendix C will be suppressed with respect to the ones containing the elements of U.

V. $l_j \to l_i \gamma$ FLAVOR VIOLATING PROCESSES AND THE μ ANOMALOUS MAGNETIC MOMENT

A. Effective Lagrangian and diagrams

The effective operators that generate the decays $l_j^- \to l_i^- \gamma$ and the lepton anomalous magnetic moment can be written as

$$\mathcal{L}_{eff} = e\frac{m_{l_j}}{2}\overline{l_i}\sigma_{\mu\nu}F^{\mu\nu}(A_{Lij}P_L + A_{Rij}P_R)l_j. \quad (29)$$

The one-loop contributions to $A_{L,R}$ in the model under consideration arise from the diagrams of Figs. 1–3:

$$A_{Lij} = A_{Lij}^S + A_{Lij}^G + A_{Lij}^Q, \quad (30)$$

$$A_{Rij} = A_{Rij}^S + A_{Rij}^G + A_{Rij}^Q. \quad (31)$$

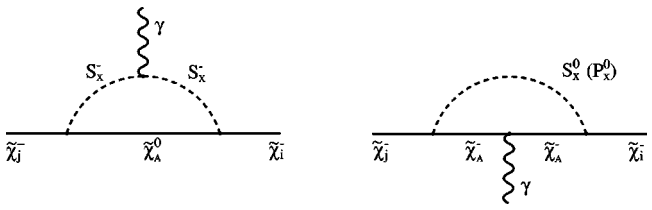

FIG. 2. Generic Feynman diagrams for $A_{L/R}^{S,ij}$.

The partial contributions in the above expressions correspond to the addition of the sets of diagrams represented in each figure:

$$A_{L,Rij}^{G}=A_{L,Rij}^{N^0-W^\pm}+A_{L,Rij}^{C^\pm-Z^0}, \tag{32}$$

$$A_{L,Rij}^{S}=A_{L,Rij}^{N^0-S^\pm}+A_{L,Rij}^{C^\pm-S^0}+A_{L,Rij}^{C^\pm-P^0}, \tag{33}$$

$$A_{L,Rij}^{Q}=A_{L,Rij}^{d\gamma-\tilde{u}}+A_{L,Rij}^{d-\tilde{u}\gamma}+A_{L,Rij}^{u\gamma-\tilde{d}}+A_{L,Rij}^{u-\tilde{d}\gamma}. \tag{34}$$

The superscripts in each contribution on the right denote the fermion and boson internal lines of the corresponding diagram. For the quarks-squarks diagrams we include the symbol γ to indicate whether the photon is attached to the fermion or the boson line. We follow the notation of [15] indicating by $S^\pm$ the eigenstates of the charged scalar mass matrix, by S^0 and P^0 the eigenstates for the sneutrino–Higgs-boson scalar mass matrices, CP even and CP odd, respectively.

The contributions to $A_{L,Rij}^{G}$ arise from the diagrams in Fig. 1. The index $A=1,\ldots,5$ corresponds to the eigenstates of the chargino-lepton mass matrix, while the indices $i,j=1,2,3$ correspond to the lepton generation indices in the limit of the MSSM with R-parity conservation. These diagrams will become the SM contribution to $\mathcal{L}_{eff}$, Eq. (29), in the limit $\epsilon_i=0$. In the case of the SM this provides the main contribution to a_μ, no contribution for charged LFV processes when neutrinos are considered massless and a very suppressed contribution for the values of m_{ν_i} compatible with the experimental limits [4].

The contributions to $A_{L/R}^{S,ij}$ arise from the three diagrams of Fig. 2, where the index X refers to the eigenstates of scalar mass matrices. $S^\pm$ are the eigenstates of the 8×8 charged Higgs-boson–slepton mass matrix and S^0,P^0 represent the eigenstates of the 5×5 neutral Higgs boson–sneutrino scalar and pseudoscalar mass matrices, respectively. In the limit where R parity is conserved these three diagrams will be combined in the two supersymmetric diagrams contributing to the $A_{L/R}$ in the MSSM. In this limit, these diagrams are flavor conserving when the soft terms are universal as given by the minimal supergravity version of the MSSM.

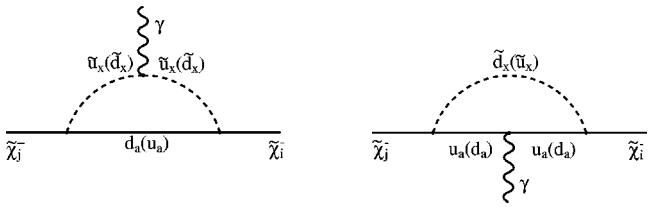

FIG. 3. Generic Feynman diagrams for $A_{L/R}^{Q,ij}$.

$A_{L/R}^{Q,ij}$ arise from the four diagrams of Fig. 3, where the indices $X=1,\ldots,6$ refer to the eigenstates of 6×6 squark mass matrices and indices $a=1,2,3$ are the quark generation indices. These diagrams are not present when R parity is conserved.

B. BR($l_j\to l_i\gamma$) for flavor violating processes

The branching ratio for the rare lepton decays $l_j\to l_i\gamma$ is given in the literature [7] and we do not repeat the derivation here. The result is

$$\mathrm{BR}(l_j^-\to l_i^-\gamma)=\frac{48\pi^3\alpha}{G_F^2}(|A_{Lij}|^2+|A_{Rij}|^2) \tag{35}$$

where the amplitudes A_{Lij} and A_{Rij} were defined in Eq. (30). The complete expressions for the amplitudes corresponding to these processes in the BRPV model are given in Appendix C. In their derivation we have neglected the mass of the outgoing fermion.

C. The muon anomalous magnetic moment

The expression for the muon anomalous magnetic moment can be obtained from the Lagrangian given in Eq. (29). One obtains [33],

$$a^\mu=\frac{(g_\mu-2)}{2}=-m_\mu^2(A_L^{\mu\mu}+A_R^{\mu\mu}). \tag{36}$$

The amplitudes $A_{L/R}^{\mu\mu}$ can also be obtained from the formulas of Appendix C by including the effect of m_μ in both external lines of the diagrams. To do that we just have to include a factor of 2 in the part of the amplitude containing the function f_P, $P=N,C,W,Z$:

$$A_{L/R}^{a_\mu}=A_{L/R}^{22}[f_P(x)\to2f_P(x)]. \tag{37}$$

VI. RESULTS

A. The parameter space

The BRPV model that we consider adds more free parameters to the ones already present in the MSSM. However, if we consider the phenomenological constraints imposed on the MSSM by the limits on the mass of the lightest neutral CP-even Higgs boson m_h, by the BR($b\to s\gamma$) and by the value of the a^μ, as well as those derived from neutrino physics on the BRPV parameters, we can narrow the space of parameters such that generic predictions for BR($\mu\to e\gamma$) and BR($\tau\to\mu\gamma$) can be made.

We assume the parameter space of the MSSM with universal soft terms and GUT unification,

$$\alpha_G, M_{GUT}, m_0, M_{1/2}, \tan\beta, \mu, B, h_E, h_U, h_D, A_0, \tag{38}$$

with the addition of the BRPV parameters,

$$\epsilon_i, B_i, v_i, \quad i=1,2,3. \tag{39}$$

A_0 is defined such that $A_I(\mathrm{GUT})=A_0\cdot h_I$, $I=U,D,E$. The quantities $\alpha_G=g_G^2/4\pi$ (g_G being the GUT gauge coupling constant) and M_{GUT} are evaluated consistently with the experimental values of $\alpha_{\mathrm{e.m.}}$, α_s, and $\sin^2\theta_W$ at m_Z. We integrate numerically the RGE's for the BRPV model, at two loops in the gauge and Yukawa couplings and at one loop in the soft terms, from M_{GUT} down to a common supersymmetric threshold $M_S\sim\sqrt{m_{\tilde{t}_1}m_{\tilde{t}_2}}$. From this energy to m_Z, the renormalization group equations (RGE's) of the SM are used.

As we explained before, the minimum conditions of the effective scalar potential allow us to express the values of μ,B,B_1,B_2,B_3 in terms of $\tan\beta,\epsilon_i,v_i$. These are evaluated at the scale M_S. The value of μ obtained at this scale is similar to the one obtained by minimizing the effective potential with the complete 1-loop MSSM contributions [34]. The 1-loop contributions arising from RP-violating terms for these parameters are comparatively much smaller.

We fix the elements of the quark Yukawa matrices at the GUT scale, consistently with the experimental values of the quark masses and the absolute values of the Cabibbo-Kobayashi-Maskawa (CKM) matrix elements. In the case of the charged leptons we have to make sure that the three lightest eigenvalues of the chargino–charged-lepton matrix are consistent with the experimental values of the charged lepton masses.

The values of m_0 and $m_{1/2}$ are chosen in the region of the parameter space favored by the considerations presented in Ref. [33], so that we can compare our results with typical predictions for the BR($\mu\to e\gamma$) in the MSSM with a seesaw mechanism, as discussed in Ref. [8]. Obviously, since our model breaks R parity, the lightest supersymmetric particle (LSP) is not a dark matter candidate and therefore the cosmological preferred areas of Ref. [33] do not apply to our study. However, the restriction of considering points in the m_0-$m_{1/2}$ plane such that $m_h>113$ GeV is the most restrictive. The SUSY contribution to a^μ [35] favors the sign of μ to be positive for the choice of SUSY parameters given below. We found that the upper bound of Eq. (47) (see below) on δa^μ is less restrictive than the one imposed by $m_h>113$ GeV. We analyze three sets of SUSY parameters,

(a) $\tan\beta=10$, $m_{1/2}=400$ GeV, $m_0=200$ GeV, $A_0=0$, $m_\nu=0.1$ eV,

(b) $\tan\beta=30$, $m_{1/2}=400$ GeV, $m_0=300$ GeV, $A_0=0$, $m_\nu=0.1$ eV,

(c) $\tan\beta=30$, $m_{1/2}=600$ GeV, $m_0=300$ GeV, $A_0=0$, $m_\nu=0.1$ eV.

The six free BRPV parameters ϵ_i,v_i reduce to three if we take into account the constraints imposed by the predictions for neutrino oscillations in this model, as given in Ref. [15]. By setting the atmospheric neutrino anomaly scale to the magnitude of the tree level nonzero value of one of the neutrinos, Eq. (22), we fix the value $\Sigma_i\Lambda_i^2$ for each SUSY point, where the Λ_i were defined in Eq. (21). We then follow the discussion of Ref. [15], where it was shown that the conditions $\Lambda_3\simeq\Lambda_2\simeq5\times\Lambda_1$ satisfy both the atmospheric neutrino anomaly mixings and the CHOOZ result [2]. We then obtain a linear relationship between each couple ϵ_i,v_i.

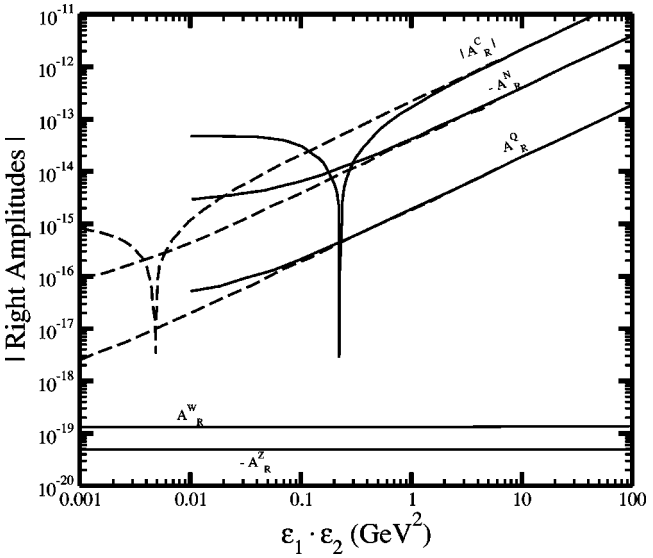

FIG. 4. Partial amplitudes A_R corresponding to the choice of parameters (b) of Sec. VI A for $\epsilon_1=-5$ GeV (solid) and $\epsilon_1=-0.1$ GeV (dash). The values of A_R^C change sign on each branch of the curve; the left one corresponds to positive values.

Therefore we study the dependence of the process under consideration on the values of $\epsilon_1,\epsilon_2,\epsilon_3$ for a neutrino mass of $m_{\nu_3}=0.1$ eV, on the upper limit of the allowed range for the atmospheric neutrino anomaly. For comparison purposes we also present some results for $m_{\nu_3}=0.05$ eV in the middle of that range, and for $m_{\nu_3}=1$ eV.

We will assign random values to ϵ_1 and ϵ_2 in the range

$$-2\times10^{-3}\ \mathrm{GeV}\geqslant\epsilon_1,\epsilon_2\geqslant-60\ \mathrm{GeV}. \tag{40}$$

However, the requirement that $m_{\nu_2}<0.01$ eV will exclude values of $|\epsilon_i|>0.1$ GeV. This will be explicitly shown in our results. The value of ϵ_3 is kept fixed since our results are not altered when it varies in the above range.

B. The branching ratio for $l_j^-\to l_i^-\gamma$

We perform a full numerical analysis with the exact diagonalization of matrices involved in the computation of branching ratios. The main contribution for BR($\mu\to e\gamma$), Eq. (35), comes from the amplitudes A_R. The partial contributions from the various diagrams listed in Eqs. (32)–(34) are displayed in Fig. 4, for the set of parameters (b). We have found that they are all independent of ϵ_3 and that they display a linear behavior as a function of the product $\epsilon_1\cdot\epsilon_2$, when this product is larger than 0.1 GeV except for the cancellation observed in $A_R^C=A_R^{C^\pm-S^0}+A_R^{C^\pm-P^0}$. The values of the amplitudes arising from the diagrams of Fig. 1 depend on the ϵ's through the Λ's which are kept fixed, and therefore remain constant. We also found the contributions of the diagrams of Fig. 3 to be of the same order of magnitude. As we can see, the sum of all of them, A_R^Q, is almost a linear function of $\epsilon_1\cdot\epsilon_2$. The amplitudes arising from the diagrams of Fig. 2 are the dominant ones. The one mediated by the neu-

tralino (A_R^N) is smaller than the dominant chargino exchange (A_R^C), except in the range where the cancellation takes place.

We can also observe in Fig. 4 that the cancellation that appears in the A_R^C depends on the value of ϵ_1. The values that we show correspond to two different choices of ϵ_1 (note that if we allowed ϵ_1 to change randomly, as we have done with the other amplitudes, the values for A_R^C would be a distribution of dots). The behavior of A_R^C cannot be attributed to an accidental cancellation between the scalar and pseudoscalar parts as one may naively expect; on the contrary both parts add constructively and almost vanish simultaneously. The behavior of that amplitude can be explained when we identify which are the particles running in the loops of Fig. 2 that are responsible for the main contributions: $X=1$, $A=1$ and $X=4$, $A=1,2$. Then we can obtain an accurate approximation for the amplitude by using the formulas given in Appendixes A, B and C. Let us consider $A_R^{C^\pm - S^0}$ since the contribution of the corresponding pseudoscalar exchange is almost identical. We get from Eq. (C4) for the dominant contributions

$$A_{R34}^{C^\pm - S^0} \approx -\frac{1}{32\pi^2}\left[\frac{1}{m_{S_1^0}^2} h_C(x_{11}) \frac{m_{\chi_1^\pm}}{m_\mu} V_{R311}^{ccs} V_{L411}^{ccs*} + \frac{1}{m_{S_4^0}^2} \sum_{A=1}^{2} h_C(x_{A4}) \frac{m_{\chi_A^\pm}}{m_\mu} V_{R3A4}^{ccs} V_{L4A4}^{ccs*}\right]. \quad (41)$$

Using the definitions of Appendix B we find,

$$V_{R311}^{ccs} V_{L411}^{ccs*} \approx -\frac{g h_\mu}{\sqrt{2}} U_{32} U_{14},$$

$$V_{R3A4}^{ccs} V_{L4A4}^{ccs*} \approx \frac{g h_\mu}{\sqrt{2}} U_{34} V_{A1} U_{A2}, \quad (42)$$

where h_μ is the Yukawa coupling of the muon. We can then write

$$A_{R34}^{C^\pm - S^0} \approx F_1 U_{32} U_{14} + F_2 U_{34} \quad (43)$$

where

$$F_1 = \frac{g h_\mu}{32\sqrt{2}\,\pi^2} \frac{1}{m_{S_1^0}^2} h_C(x_{11}) \frac{m_{\chi_1^\pm}}{m_\mu},$$

$$F_2 = -\frac{g h_\mu}{32\sqrt{2}\,\pi^2} \frac{1}{m_{S_4^0}^2} \sum_{A=1}^{2} h_C(x_{A4}) \frac{m_{\chi_A^\pm}}{m_\mu} V_{A1} U_{A2}. \quad (44)$$

The quantities F_1 and F_2 are independent of the BRPV parameters ϵ_i and can be evaluated given the SUSY parameters. The dependence of the amplitude $A_{R34}^{C^\pm - S^0}$ on ϵ_i comes from the matrix elements U_{32}, U_{14} and U_{34}. Using Appendix A we can find approximate expressions for these matrix elements that display this dependence explicitly. We get

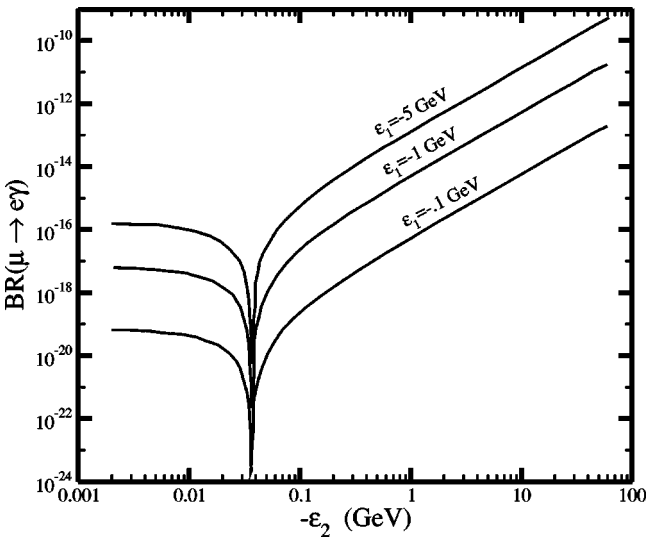

FIG. 5. BR($\mu \to e\gamma$) vs $-\epsilon_2$ for $\epsilon_1 = -0.1, -1, -5$ GeV for case (b).

$$U_{34} \approx -\frac{\epsilon_1 \epsilon_2}{\mu^2} + \frac{\epsilon_1 \Lambda_2}{v_d \mu^2},\ U_{32} \approx \frac{\epsilon_1}{\mu},\ U_{14} \approx -U_{12}^L \frac{\epsilon_2}{\mu}. \quad (45)$$

Hence we can find the value of ϵ_2 at which $A_R^C \simeq 0$,

$$\epsilon_2 \approx \frac{\Lambda_2 F_2 / v_d}{F_2 + F_1 U_{12}^L}. \quad (46)$$

The position of the cancellation changes, with the value of the SUSY parameters and also with the value of Λ_2, as we can see from Eq. (46). This explains the qualitative changes we find in Figs. 5–10.

Some of the amplitudes contributing to the BR($\mu \to e\gamma$) presented above have been previously discussed in Refs. [9,11]. We agree with Ref. [11] in that the main contribution arises from A_R^C except for the values of parameters affected

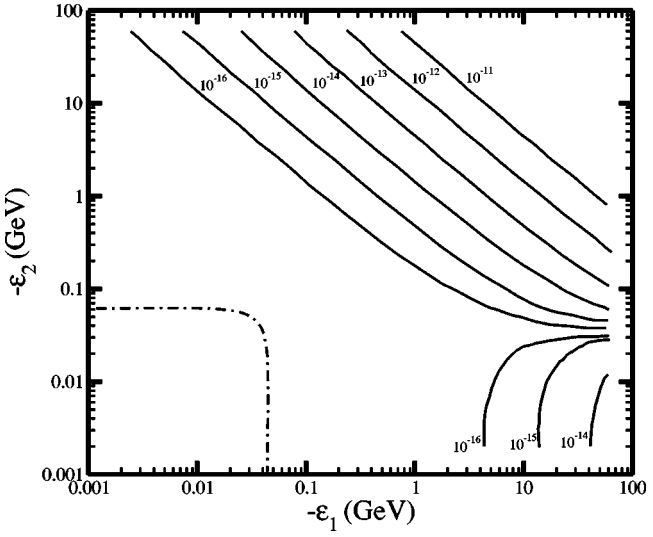

FIG. 6. Contour plot for BR($\mu \to e\gamma$) in ϵ_1-ϵ_2 plane for case (b). The dash lines correspond to $m_{\nu_2} = 0.01$ eV.

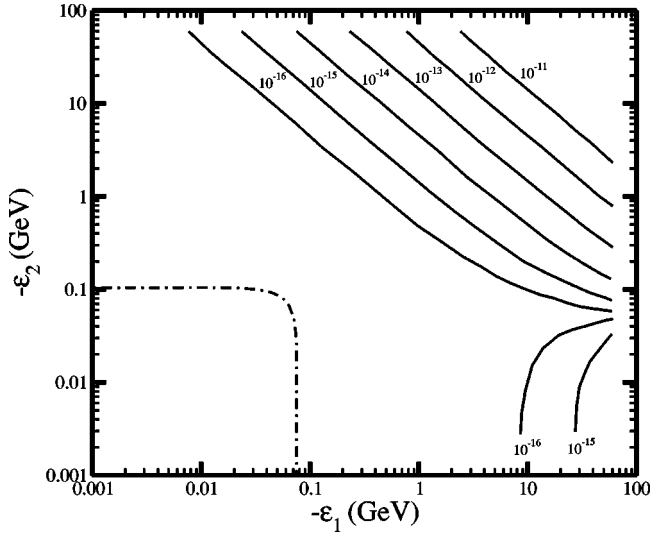

FIG. 7. Contour plot for BR($\mu \to e\gamma$) in ϵ_1-ϵ_2 plane for case (c). The dashed lines correspond to $m_{\nu_2} = 0.01$ eV.

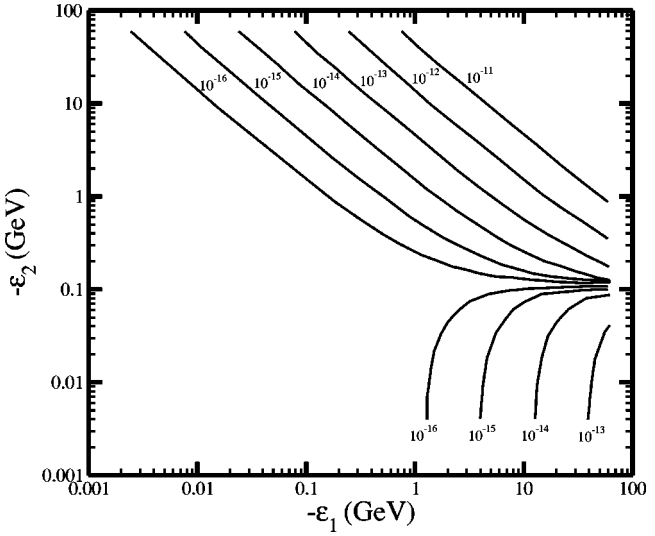

FIG. 9. Same as Fig. 6, case (b) for $m_{\nu_3} = 1$ eV.

by the cancellation mentioned above. However we find smaller values for A_R^Q than the ones quoted in [9].

The contribution of A_L to the branching ratio is negligible compared with A_R, due to the fact that the matrix U is replaced by V with suppressed mixings. This holds even for the element V_{34}. As we can see in Appendix A this element is determined by V_R which is obtained in a similar way as V_L for the matrix U. However, we observe that the main contribution to V_{34} is suppressed by a factor m_e/m_μ with respect to the corresponding one in U_{34}.

Figure 5 shows the impact of the cancellation in A_R^C on the predictions of BR($\mu \to e\gamma$) for the choice of parameters (b). As we can deduce from Eq. (46) the value of the ϵ_2 at which the cancellation in A_R^C takes place depends on the values of the SUSY parameters. This determines the shape of the curves of constant BR in Figs. 6–10. Since the main contribution comes from the chargino mediated diagram of Fig. 2, we can expect that the BR increases with $\tan\beta$ and decreases as $m_{1/2}$ grows. The increase of m_0 produces the same qualitative effect as the increase of $m_{1/2}$; however, it has a lower impact on the BR than the changes in $m_{1/2}$.

Our results can be compared with the predictions of a model based on the MSSM with a seesaw mechanism presented in Ref. [8], where the results for BR($\mu \to e\gamma$) are of order 10^{-13} for case (a) and between 10^{-12} and 10^{-13} for (b) and (c). If we observe our predictions for case (b), Fig. 6, we can see that the model predicts ratios of 10^{-11}–10^{-13} for values of $|\epsilon_1|$ and $|\epsilon_2|$ ranging from 1 to 10 GeV (independently of the value of ϵ_3). Values in the range of 0.1 to 1 GeV would lead to rates of order 10^{-14}–10^{-16}, still interesting for the next generation experiments [25,26]. Similarly, the window of $0.1 < -\epsilon_1, -\epsilon_2 < 1$ GeV is crossed only by the 10^{-16} line in case (c) and by lines below this value for case (a). Such values of $|\epsilon_i|$ are however excluded if one takes into account the constraint coming from the solar neu-

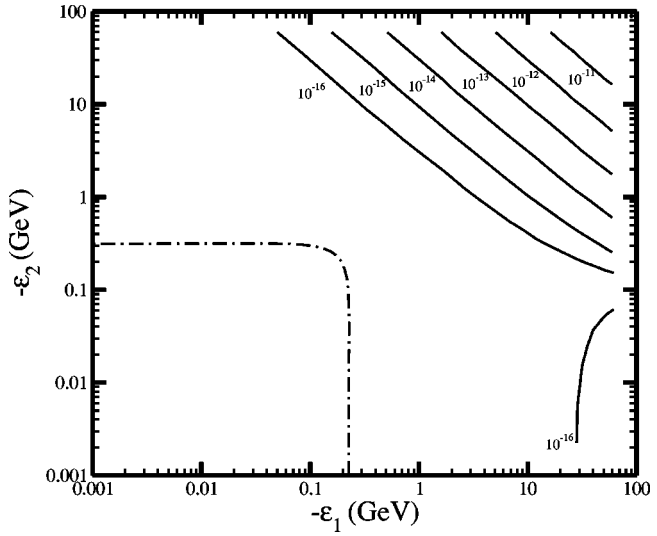

FIG. 8. Same as Fig. 6 for case (a).

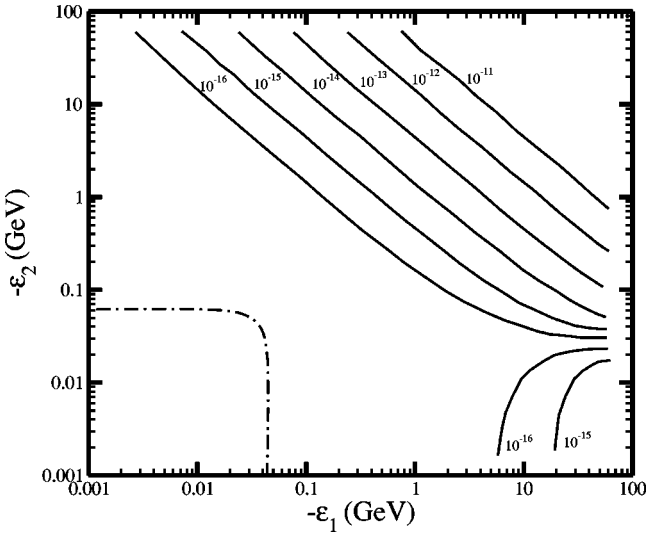

FIG. 10. Same as Fig. 6, case (b) for $m_{\nu_3} = 0.05$ eV.

TABLE I. Contributions to a_μ from the graphs in Figs. 1–3 (in units of 10^{-10}). Cases (a)–(c) refer to the choices of parameters given in Sec. VI A. See Sec. V for details of the notation.

	$a_\mu^{\tilde{\chi}^+}$	$a_\mu^{\tilde{\chi}^0}$	a_μ^q	$\delta a_\mu^{\tilde{\chi}^+}$(RPV)	$\delta a_\mu^{\tilde{\chi}^0}$(RPV)	δa_μ^Z(RPV)	δa_μ^W(RPV)
(a)	9.6	0.45	-1.5×10^{-4}	7.5×10^{-2}	6.1×10^{-3}	-0.25	0.51
(b)	25.8	-1.1	-1.5×10^{-3}	0.35	2.5×10^{-2}	-0.28	0.52
(c)	13.8	0.19	-4.1×10^{-4}	0.11	1.9×10^{-2}	-0.14	0.28

trino mass scale. This is shown in Figs. 6, 7 and 8, where the dashed line gives the upper limit on $|\epsilon_i|$ as obtained from Eq. (23) for the requirement that $m_{\nu_2}<0.01$ eV.

In these figures we can appreciate that the parameters that enhance the ratios also make m_{ν_2} larger. From Eq. (23) we can observe that m_{ν_2} increases with $\tan\beta$ (through the dependence on h_b) and decreases as the μ term increases (i.e. with $m_{1/2}$ and m_0). Furthermore, since we have chosen the Λ parameters to be related, m_{ν_2} is proportional to a combination of ϵ_i^2 with no accidental cancellation among them. Therefore we cannot find suitable values for $\tan\beta$, $m_{1/2}$ and m_0, such that we can find an overlapping of areas with $m_{\nu_2}<0.01$ eV and $\mathrm{BR}(\mu\to e\gamma)>10^{-16}$.

In Figs. 9 and 10 we consider $m_{\nu_3}=0.05$ eV and $m_{\nu_3}=1$ eV both for case (b). This decreases (increases) the values of the Λ's by about a factor of $\sqrt{2}$ ($\sqrt{10}$), respectively. By looking at the parametrization of the matrix U in Appendix A we can infer that these changes in the Λ's do not have a decisive impact on the $\mu\to e\gamma$ rates. The reason for this is that the dominant contributions to $A_{R34}^{C^\pm-S^0,P^0}$ are determined by the matrix Ω_L and its elements that depend explicitly on the ϵ's are much larger than the ones containing Λ's (at least for values of ϵ's leading to relevant ratios). However, the position of the cancellation on $A_{R34}^{C^\pm-S^0}$ depends on Λ_2 as we can see in Eq. (46) and it therefore determines the changes in the figures. The changes in the Λ's have only a direct impact on the smaller contributions, such as the ones arising from the diagrams of Fig. 1 and on the A_L, whose size is controlled by the elements of Ω_R, which, as we have said, are several orders of magnitude below the main contribution coming from Ω_L.

The predictions for $\mathrm{BR}(\tau\to\mu\gamma)$ that we obtain with this model are of the same order as those for $\mathrm{BR}(\mu\to e\gamma)$, the reason being that we have assumed the Λ's to be of the same order of magnitude, as is required to explain neutrino oscillations. The results in this case are independent of ϵ_1. If we consider values for ϵ_2 and ϵ_3 in the same range as in Fig. 6 we obtain similar curves. This result contrasts with the LFV results on the framework of the *R*-parity conserving MSSM, where $\mathrm{BR}(\mu\to e\gamma)$ is typically suppressed by several orders of magnitude with respect to $\mathrm{BR}(\tau\to\mu\gamma)$. In this case the hierarchy of Yukawa couplings makes a distinction between the two processes.

We conclude therefore that the values of the parameters of the BRPV model that successfully explain the solar and atmospheric neutrino data [15] predict rates for $\mu\to e\gamma$, $\tau\to\mu\gamma$ and $\tau\to e\gamma$ that are well below the current limits as well as those of planned experiments.

C. The muon anomalous magnetic moment

The difference in the value of the muon anomalous magnetic moment found in the BNL E821 measurement [36] with respect to the SM prediction, which originally was considered to be 2.6σ, is now reduced to 1.6σ after a theoretical error was corrected [37]. When the 2σ range is considered, the allowed values for contributions beyond the SM become

$$-6\times10^{-10}\leqslant\delta a_\mu\equiv a_\mu^{expt}-a_\mu^{SM}\leqslant58\times10^{-10}. \qquad (47)$$

Several studies [33] indicate that the MSSM extension of the SM can account for this discrepancy. When *R* parity is broken the SUSY particles are allowed to enter in the SM diagrams (Fig. 1) and conversely the SM particles run in the SUSY loops (Figs. 2 and 3).

The contribution due to the *R*-parity violating operators to δa_μ is obtained by subtracting from the amplitudes arising from Fig. 1 $[\delta a_\mu^Z(\mathrm{RPV}),\delta a_\mu^W(\mathrm{RPV})]$ and Fig. 2 $[\delta a_\mu^{\tilde{\chi}^\pm}(\mathrm{RPV}),\delta a_\mu^{\tilde{\chi}^0}(\mathrm{RPV})]$ the contribution of the SM and the MSSM, respectively (which are obtained in the limit of vanishing ϵ_i's). The contribution from Fig. 3 (a_μ^q) is not present in the MSSM. All these contributions are found to be small when the *R*-parity violating terms are associated with neutrino masses of experimental interest.

In Table I we show the different contributions to δa_μ for the selected values of m_0, $m_{1/2}$ and $\tan\beta$ discussed in Sec. VI A. The main contributions to δa_μ arise basically from the MSSM components of the diagrams in Fig. 2 ($a_\mu^{\tilde{\chi}^+}$,$a_\mu^{\tilde{\chi}^0}$). The contribution from BRPV operators just adds a small percentage to the total values arising from physics beyond the SM. The values that we show correspond to the maximum value obtained in the conditions for the ϵ parameters described in Sec. VI A, when we allow $|\epsilon_1|,|\epsilon_2|$ to range from 0 to 60 GeV (the result is almost independent of the value of ϵ_3).

VII. CONCLUSIONS

We studied the LFV in one-loop induced rare processes $l_j\to l_i\gamma$, $i\neq j$, in SUSY models with bilinear *R*-parity violation. In this context, the *R*-parity violating interactions can explain the neutrino masses and mixings without adding new fields to the particle content of the MSSM which represent an appealing alternative to the seesaw mechanism. In this work we addressed the question of whether neutrino masses in the sub-eV range can be compatible with rates for charged

LFV processes of experimental interest.

We have performed an exhaustive study of the interactions and of the SUSY parameters involved in the processes $l_j \to l_i \gamma$, $i \neq j$, and contributing to the muon anomalous magnetic moment. For the case of rare decays we find the diagram mediated by the Higgs-boson–sneutrino scalars to be dominant. Contributions arising from diagrams including lepton-squark and lepton-gauge-boson vertices, possible in this model, are very suppressed in the range of neutrino masses considered in this work. Regarding a_μ, the additional contributions introduced by the *R*-parity violating interactions modify by a small percentage the value obtained in the MSSM limit.

As in a previous analysis [11] we find BR($\mu \to e\gamma$) to be very sensitive to the product $\epsilon_1 \cdot \epsilon_2$. However, the presence of a cancellation in the main amplitude contributing to this process (which we have analyzed in detail through an accurate parametrization of the matrices U,V), makes our contour plots sensitive to the values of ϵ_1 and ϵ_2 in most of our examples. The rate increases with $\tan\beta$ as it is the case in the MSSM with ''seesaw'' mechanism. However as the one-loop induced neutrino masses will also grow with $\tan\beta$, the requirement that Δm^2_{12} is compatible with the solar neutrino data excludes the region in parameter space where the BR($\mu \to e\gamma$) could be of experimental interest. On the other hand the rates for $\tau \to \mu\gamma$ found in our study are of the same order as the ones for $\mu \to e\gamma$, and therefore also out of the experimental range.

Unlike the situation in these models, the rates for $\tau \to \mu\gamma$ found in our study are of the same order as the ones for $\mu \to e\gamma$, and therefore out of the experimental range.

To conclude, we must say that the obtained results for $\mu \to e\gamma$ show us that if the BRPV model is the explanation for both the solar and atmospheric neutrino oscillations, the predicted LFV will not be testable at PSI [25] or at PRISM [26]. The correlations of the BRPV parameters with the neutralino decays, as proposed in Ref. [38], will remain the main test of the model.

ACKNOWLEDGMENTS

This project was supported in part by the TMR Network of the EC under contract HPRN-CT-2000-00148. D.F.C. and M.E.G. acknowledge support from the ''Fundação para a Ciência e Tecnologia'' under contracts PRAXIS XXI/BD/9416/96 and SFRH/BPD/5711/2001 respectively. We thank P. Nogueira for useful discussions.

APPENDIX A: CHARGINO–CHARGED-LEPTON MASS MATRIX

The chargino–charged-lepton mass matrix, in the basis of of Eq. (24), takes the form

$$M_C = \begin{bmatrix} M_{\chi^\pm} & E' \\ E & M_E \end{bmatrix}, \tag{A1}$$

where $M_E = (1/\sqrt{2}) v_d h_E$ is the charged lepton mass matrix and $M_{\chi^\pm}$ is the usual MSSM chargino mass matrix,

$$M_{\chi^\pm} = \begin{bmatrix} M_2 & (1/\sqrt{2}) g v_u \\ (1/\sqrt{2}) g v_d & \mu \end{bmatrix}. \tag{A2}$$

The submatrix E is

$$E = \begin{bmatrix} (1/\sqrt{2}) g v_1 & -\epsilon_1 \\ (1/\sqrt{2}) g v_2 & -\epsilon_2 \\ (1/\sqrt{2}) g v_3 & -\epsilon_3 \end{bmatrix} \tag{A3}$$

and E' can be written as $E' = -v \cdot h_E$, where v is defined as

$$v = \begin{bmatrix} 0 & 0 & 0 \\ v_1/\sqrt{2} & v_2/\sqrt{2} & v_3/\sqrt{2} \end{bmatrix}. \tag{A4}$$

As the *R*-parity breaking parameters are small compared with the SUSY scale, it is possible to have an approximate diagonalization of M_C. This will be very useful in understanding the numerical results as we can have approximate analytical formulas. This approximate diagonalization is obtained by using the following parametrization, introduced in Refs. [22,32], for U^* and $V^\dagger$:

$$U^* = \begin{bmatrix} U_L^* & 0 \\ 0 & V_L \end{bmatrix} \begin{bmatrix} 1 - \frac{1}{2}\Omega_L^\dagger \Omega_L & \Omega_L^\dagger \\ -\Omega_L & 1 - \frac{1}{2}\Omega_L \Omega_L^\dagger \end{bmatrix}, \tag{A5}$$

$$V^\dagger = \begin{bmatrix} 1 - \frac{1}{2}\Omega_R^\dagger \Omega_R & -\Omega_R^\dagger \\ \Omega_R & 1 - \frac{1}{2}\Omega_R \Omega_R^\dagger \end{bmatrix} \begin{bmatrix} U_R^\dagger & 0 \\ 0 & V_R^\dagger \end{bmatrix}, \tag{A6}$$

where $U_{L,R}$ are the MSSM rotation matrices,

$$U_L^* M_{\chi^\pm} U_R^\dagger = M_{\chi^\pm}^{diag}. \tag{A7}$$

The matrices $\Omega_{L,R}$ and $V_{L,R}$ are to be determined from the unitarity of U and V, and from the defining condition

$$U^* M_C V^\dagger = \begin{bmatrix} M_{\chi^\pm}^{diag} & 0 \\ 0 & M_E^{diag} \end{bmatrix}. \tag{A8}$$

In the literature [22,32], the matrices $\Omega_{L,R}$ and $V_{L,R}$ were obtained in the approximation $E' = 0$. However we discovered that this approximation was not good enough to explain our numerical results. So we rederived the expressions for these matrices without neglecting E'. We get the following expressions for $\Omega_{L,R}$:

$$\Omega_L = E M^{-1}_{\chi^\pm} = \frac{1}{\det(M_{\chi^\pm})} \times \begin{bmatrix} \frac{g}{\sqrt{2}}\Lambda_1 & -\frac{1}{\mu}\left[\epsilon_1 \det(M_{\chi^\pm}) + \frac{1}{2}g^2 v_u \Lambda_1\right] \\ \frac{g}{\sqrt{2}}\Lambda_2 & -\frac{1}{\mu}\left[\epsilon_2 \det(M_{\chi^\pm}) + \frac{1}{2}g^2 v_u \Lambda_2\right] \\ \frac{g}{\sqrt{2}}\Lambda_3 & -\frac{1}{\mu}\left[\epsilon_3 \det(M_{\chi^\pm}) + \frac{1}{2}g^2 v_u \Lambda_3\right] \end{bmatrix}, \tag{A9}$$

$$\Omega_R = (E'^\dagger + M_e^\dagger E M^{-1}_{\chi^\pm})(M^{-1}_{\chi^\pm})^T = h_E^\dagger \left(-v^\dagger + \frac{1}{\sqrt{2}} v_d \Omega_L \right)(M^{-1}_{\chi^\pm})^T$$

$$= \frac{1}{\det(M_{\chi^\pm})} \times \begin{bmatrix} \frac{g}{\sqrt{2}}(M_E)_{i1}\Lambda_i & -\frac{M_2}{v_d}(M_E)_{i1}\Lambda_i \\ \frac{g}{\sqrt{2}}(M_E)_{i2}\Lambda_i & -\frac{M_2}{v_d}(M_E)_{i2}\Lambda_i \\ \frac{g}{\sqrt{2}}(M_E)_{i3}\Lambda_i & -\frac{M_2}{v_d}(M_E)_{i3}\Lambda_i \end{bmatrix} \times (M^{-1}_{\chi^\pm})^T, \tag{A10}$$

where summation over $i=1,2,3$ is implied in each matrix element. The expression for Ω_L coincides with the one found in the literature but the expression for Ω_R is different. For $V_{L,R}$ we found that instead of the relation [22,32]

$$V_L M_E V_R^\dagger = M_E^{diag} \tag{A11}$$

they should satisfy

$$V_L \left(M_E - \Omega_L E' - \frac{1}{2}\Omega_L \Omega_L^T M_E \right) V_R^\dagger = M_E^{diag}. \tag{A12}$$

For a general form of the matrix M_E it will be difficult to have an explicit form for $V_{L,R}$. However, for the case that we consider, where the matrix M_E is diagonal, we can obtain an analytical approximate expression for these matrices,

$$V_{L,R} \simeq \begin{bmatrix} 1 & \eta_{12}^{L,R} & \eta_{13}^{L,R} \\ -\eta_{12}^{*\,L,R} & 1 & \eta_{23}^{L,R} \\ -\eta_{13}^{*\,L,R} & -\eta_{23}^{*\,L,R} & 1 \end{bmatrix} \tag{A13}$$

where

$$\eta_{ij}^L = \frac{\epsilon_i \epsilon_j}{2\mu^2}\frac{m_i^2+m_j^2}{m_i^2-m_j^2} + \frac{\epsilon_i \Lambda_j}{\mu^2 v_d}\left[\frac{g^2 v_u v_d}{2\det(M_{\chi^\pm})} - \frac{m_j^2}{m_i^2-m_j^2}\right] + \frac{\epsilon_j \Lambda_i}{\mu^2 v_d}\left[-\frac{g^2 v_u v_d}{2\det(M_{\chi^\pm})} - \frac{m_i^2}{m_i^2-m_j^2}\right] - \frac{\Lambda_i \Lambda_j}{\det(M_{\chi^\pm})\,\mu^2}\frac{g^2 v_u}{v_d}\frac{m_i^2+m_j^2}{m_i^2-m_j^2}, \tag{A14}$$

$$\eta_{ij}^R = \frac{\epsilon_i \epsilon_j}{\mu^2}\frac{m_i m_j}{m_i^2-m_j^2} - \frac{\epsilon_i \Lambda_j}{\mu^2 v_d}\frac{m_i m_j}{m_i^2-m_j^2} - \frac{\epsilon_j \Lambda_i}{\mu^2 v_d}\frac{m_i m_j}{m_i^2-m_j^2} - \frac{\Lambda_i \Lambda_j}{\det(M_{\chi^\pm})\mu^2}\frac{2\,g^2 v_u}{v_d}\frac{m_i m_j}{m_i^2-m_j^2}, \tag{A15}$$

and m_i are the charged lepton physical masses.

Putting everything together we can find analytical expressions for the matrix U that will be useful in explaining our results. We get

$$U^*_{2+i,1} \simeq -\frac{g}{\sqrt{2}}\frac{\Lambda_i}{\det(M_{\chi^\pm})}, \tag{A16}$$

$$U^*_{2+i,2} \simeq -\Omega_{Li2} \simeq \frac{\epsilon_i}{\mu}, \tag{A17}$$

$$U^*_{1,2+i} \simeq U^*_{L12}\Omega_{Li2} \simeq -U^*_{L12}\frac{\epsilon_i}{\mu}, \tag{A18}$$

$$U^*_{2,2+i} \simeq U^*_{L22}\Omega_{Li2} \simeq -U^*_{L22}\frac{\epsilon_i}{\mu}, \tag{A19}$$

$$U^*_{2+i,2+j} \simeq \left(V_L - \frac{1}{2}\Omega_L \Omega_L^T \right)_{ij}. \tag{A20}$$

For further reference we give the approximate expression for $U^*_{3,4}$. We get

$$U^*_{34} \simeq -\frac{\epsilon_1 \epsilon_2}{\mu^2} + \frac{\epsilon_1 \Lambda_2}{\mu^2 v_d} - \frac{g v_u \epsilon_2 \Lambda_1}{\det(M_{\chi^\pm})\mu^2} \simeq -\frac{\epsilon_1 \epsilon_2}{\mu^2} + \frac{\epsilon_1 \Lambda_2}{\mu^2 v_d} \tag{A21}$$

where we have assumed that the parameters are in the ranges described in Sec. VI A.

APPENDIX B: THE COUPLINGS

The relevant part of the Lagrangian, using four component spinor notation, is

$$\mathcal{L}=+\overline{\chi_i^-}(V_{LiAX}^{ccs}P_L+V_{RiAX}^{ccs}P_R)\chi_A^- S_X^0+\overline{\chi_i^-}(V_{LiAX}^{ccp}P_L+V_{RiAX}^{ccp}P_R)\chi_A^- P_X^0+\overline{\chi_i^-}\gamma^\mu(V_{LiA}^{ccZ}P_L+V_{RiA}^{ccZ}P_R)\chi_A^- Z_\mu^0$$
$$+[\overline{\chi_i^-}(V_{LiAX}^{cns}P_L+V_{RiAX}^{cns}P_R)\chi_A^0 S_X^- +\overline{\chi_i^-}(V_{LiAX}^{cd\tilde{u}}P_L+V_{RiAX}^{cd\tilde{u}}P_R)d_A\tilde{u}_X^*+\overline{\chi_i^+}(V_{LiAX}^{cu\tilde{d}}P_L+V_{RiAX}^{cu\tilde{d}}P_R)u_A\tilde{d}_X^*$$
$$+\overline{\chi_i^-}\gamma^\mu(V_{LiA}^{cnW}P_L+V_{RiA}^{cnW}P_R)\chi_A^0 W_\mu^- +\text{H.c.}]. \tag{B1}$$

The definition of these couplings is given in the following sections. These definitions extend those of Ref. [15], whose conventions we follow.

1. Chargino-neutralino charged scalars

$$V_{LiAX}^{cns}=-\rho_A\Bigg[gR_{X2}^{S^\pm}\left(\frac{1}{\sqrt{2}}N_{A2}^*V_{i2}^*+N_{A4}^*V_{i1}^*\right)$$
$$+\frac{g'}{\sqrt{2}}(R_{X2}^{S^\pm}N_{A1}^*V_{i2}^*+2R_{X5+\alpha}^{S^\pm}V_{i2+\alpha}^*N_{A1}^*)$$
$$+(R_{X2+\alpha}^{S^\pm}h_E^{\alpha\beta}N_{A3}^*-R_{X1}^{S^\pm}N_{A4+\alpha}^*h_E^{\alpha\beta})V_{i2+\beta}^*\Bigg], \tag{B2}$$

$$V_{RiAX}^{cns}=\eta_i\Bigg[gR_{X1}^{S^\pm}\left(\frac{1}{\sqrt{2}}N_{A2}U_{i2}-N_{A3}U_{i1}\right)$$
$$+gR_{X2+\alpha}^{S^\pm}\left(\frac{1}{\sqrt{2}}U_{i2+\alpha}N_{A2}-N_{A4+\alpha}U_{i1}\right)$$
$$+\frac{g'}{\sqrt{2}}(R_{X1}^{S^\pm}N_{A1}U_{i2}+R_{X2+\alpha}^{S^\pm}U_{i2+\alpha}N_{A1})$$
$$+(U_{i2}N_{A4+\alpha}-N_{A3}U_{i2+\alpha})h_E^{\alpha\beta}R_{X5+\beta}^{S^\pm}\Bigg] \tag{B3}$$

where the indices have the following ranges: $A=1,\ldots,7$, $i=1,\ldots,5$, $\alpha,\beta=1,\ldots,3$ and ρ_A (η_i) are the signs of the neutralinos (charginos) as they are obtained from the numerical evaluation of the eigenvalues [15].

2. Chargino-chargino *CP* even neutral scalars

$$V_{LiAX}^{ccs}=-\eta_A\frac{1}{\sqrt{2}}[g(R_{X1}^{S^0}U_{A2}^*V_{i1}^*+R_{X2}^{S^0}U_{A1}^*V_{i2}^*$$
$$+R_{X2+\alpha}^{S^0}U_{A2+\alpha}^*V_{i1}^*)+(R_{X1}^{S^0}U_{A2+\alpha}^*$$
$$-U_{A2}^*R_{X2+\alpha}^{S^0})h_E^{\alpha\beta}V_{i2+\beta}^*], \tag{B4}$$

$$V_{RiAX}^{ccs}=V_{LAiX}^{ccs*}. \tag{B5}$$

3. Chargino-chargino *CP* odd neutral scalars

$$V_{LiAX}^{ccp}=i\eta_A\frac{1}{\sqrt{2}}[g(R_{X1}^{P^0}U_{A2}^*V_{i1}^*+R_{X2}^{P^0}U_{A1}^*V_{i2}^*$$
$$+R_{X2+\alpha}^{P^0}U_{A2+\alpha}^*V_{i1}^*)+(U_{A2}^*R_{X2+\alpha}^{P^0}$$
$$-R_{X1}^{S^0}U_{A2+\alpha}^*)h_E^{\alpha\beta}V_{i2+\beta}^*], \tag{B6}$$

$$V_{RiAX}^{ccp}=V_{LAiX}^{ccp*}. \tag{B7}$$

4. Chargino-neutralino-$W^\pm$

$$V_{LiA}^{cnW}=-\eta_i\rho_A g\left[N_{A2}^*U_{i1}+\frac{1}{\sqrt{2}}(N_{A3}^*U_{i2}+N_{A4+\alpha}^*U_{i2+\alpha})\right], \tag{B8}$$

$$V_{RiA}^{cnW}=g\left[\frac{1}{\sqrt{2}}N_{A4}V_{i2}^*-N_{A2}V_{i1}^*\right]. \tag{B9}$$

5. Chargino-chargino-Z^0

$$V_{LiA}^{ccZ}=\eta_i\eta_A\frac{g}{\cos\theta_W}\left[\frac{1}{2}U_{i1}U_{A1}^*+\left(\frac{1}{2}-\sin^2\theta_W\right)\delta_{iA}\right], \tag{B10}$$

$$V_{RiA}^{ccZ}=\frac{g}{\cos\theta_W}\left[V_{i1}^*V_{A1}+\frac{1}{2}V_{i2}^*V_{A2}-\sin^2\theta_W\delta_{iA}\right]. \tag{B11}$$

6. Chargino–quark down–squark up

$$V_{LiAX}^{cd\tilde{u}}=\eta_A^d[-gV_{i1}^*R_{X\alpha}^{\tilde{u}}R_{LA\alpha}^{d*}+V_{i2}^*R_{LA\alpha}^{d*}h_U^{\alpha\beta}R_{X3+\beta}^{\tilde{u}}], \tag{B12}$$

$$V_{RiAX}^{cd\tilde{u}}=\eta_i[U_{i2}R_{X\alpha}^{\tilde{u}}h_D^{\alpha\beta}R_{RA\beta}^d]. \tag{B13}$$

7. Chargino–quark up–squark down

$$V_{LiAX}^{cu\tilde{d}}=\eta_i\eta_A^u[-gU_{i1}^*R_{X\alpha}^{\tilde{d}}R_{LA\alpha}^{u*}+U_{i2}^*R_{LA\alpha}^{u*}h_D^{\alpha\beta}R_{X3+\beta}^{\tilde{d}}], \tag{B14}$$

$$V_{RiAX}^{cu\tilde{d}}=V_{i2}R_{X\alpha}^{\tilde{d}}h_U^{\alpha\beta}R_{RA\beta}^{u*}. \tag{B15}$$

APPENDIX C: AMPLITUDES

We collect here the various amplitudes corresponding to the diagrams of Figs. 1–3. In these amplitudes the mass of

the outgoing fermion was neglected. We give only the amplitudes A_L because the A_R can be obtained from these with the substitution rule

$$A_{Rij}=A_{Lij}(L/R\to R/L). \tag{C1}$$

1. Neutralinos–charged-scalars

$$A_{Lij}^{N^0\text{-}S^\pm}=\sum_{A=1}^{5}\sum_{X=1}^{8}\frac{1}{32\pi^2}\frac{1}{m^2_{S^\pm_X}}\left[f_N(x_{AX})V^{cns}_{LiAX}V^{cns*}_{LjAX}+h_N(x_{AX})\frac{m_{\chi^0_A}}{m_{l_j}}V^{cns}_{LiAX}V^{cns*}_{RjAX}\right] \tag{C2}$$

with $x_{AX}=(m_{\chi^0_A}/m_{S^\pm_X})^2$ and the functions f_N, h_N given by

$$f_N(x)=\frac{1-6x+3x^2+2x^3-6x^2\ln x}{6(1-x)^4},$$

$$h_N(x)=\frac{1-x^2+2x\ln x}{(1-x)^3}. \tag{C3}$$

2. Charginos–*CP* even neutral scalars

$$A_{Lij}^{C^\pm\text{-}S^0}=\sum_{A=1}^{5}\sum_{X=1}^{5}-\frac{1}{32\pi^2}\frac{1}{m^2_{S^0_X}}\left[f_C(x_{AX})V^{ccs}_{LiAX}V^{ccs*}_{LjAX}+h_C(x_{AX})\frac{m_{\chi^\pm_A}}{m_{l_j}}V^{ccs}_{LiAX}V^{ccs*}_{RjAX}\right] \tag{C4}$$

with $x_{AX}=(m_{\chi^\pm_A}/m_{S^0_X})^2$ and the functions f_C, h_C given by

$$f_C(x)=\frac{2+3x-6x^2+x^3+6x\ln x}{6(1-x)^4},$$

$$h_C(x)=\frac{-3+4x-x^2-2\ln x}{(1-x)^3}. \tag{C5}$$

3. Charginos–*CP* odd neutral scalars

$$A_{Lij}^{C^\pm\text{-}P^0}=\sum_{A=1}^{5}\sum_{X=1}^{5}-\frac{1}{32\pi^2}\frac{1}{m^2_{P^0_X}}\left[f_C(x_{AX})V^{ccp}_{LiAX}V^{ccp*}_{LjAX}+h_C(x_{AX})\frac{m_{\chi^\pm_A}}{m_{l_j}}V^{ccp}_{LiAX}V^{ccp*}_{RjAX}\right] \tag{C6}$$

with $x_{AX}=(m_{\chi^\pm_A}/m_{P^0_X})^2$.

4. Quarks-squarks

$$A_{Lij}^{d\gamma\text{-}\tilde{u}}=\sum_{A=1}^{3}\sum_{X=1}^{6}3\left(-\frac{1}{3}\right)\frac{1}{32\pi^2 m^2_{\tilde{u}_X}}\left[f_C(x_{AX})V^{cd\tilde{u}}_{LiAX}V^{cd\tilde{u}*}_{LjAX}+h_C(x_{AX})\frac{m_{d_A}}{m_{l_j}}V^{cd\tilde{u}}_{LiAX}V^{cd\tilde{u}*}_{RjAX}\right] \tag{C7}$$

with $x_{AX}=(m_{d_A}/m_{\tilde{u}_X})^2$.

$$A_{Lij}^{u\gamma\text{-}\tilde{d}}=\sum_{A=1}^{3}\sum_{X=1}^{6}3\left(\frac{2}{3}\right)\frac{1}{32\pi^2 m^2_{\tilde{d}_X}}\left[f_C(x_{AX})V^{cu\tilde{d}}_{RiAX}V^{cu\tilde{d}*}_{RjAX}+h_C(x_{AX})\frac{m_{u_A}}{m_{l_j}}V^{cu\tilde{d}}_{RiAX}V^{cu\tilde{d}*}_{LjAX}\right] \tag{C8}$$

with $x_{AX}=(m_{u_A}/m_{\tilde{d}_X})^2$.

$$A_{Lij}^{d\text{-}\tilde{u}\gamma}=\sum_{A=1}^{3}\sum_{X=1}^{6}3\left(\frac{2}{3}\right)\frac{1}{32\pi^2 m^2_{\tilde{u}_X}}\left[f_N(x_{AX})V^{cd\tilde{u}}_{LiAX}V^{cd\tilde{u}*}_{LjAX}+h_N(x_{AX})\frac{m_{d_A}}{m_{l_j}}V^{cd\tilde{u}}_{LiAX}V^{cd\tilde{u}*}_{RjAX}\right] \tag{C9}$$

with $x_{AX}=(m_{d_A}/m_{\tilde{u}_X})^2$.

$$A_{Lij}^{u\text{-}\tilde{d}\gamma}=\sum_{A=1}^{3}\sum_{X=1}^{6}3\left(-\frac{1}{3}\right)\frac{1}{32\pi^2 m^2_{\tilde{d}_X}}\left[f_N(x_{AX})V^{cu\tilde{d}}_{RiAX}V^{cu\tilde{d}*}_{RjAX}+h_N(x_{AX})\frac{m_{u_A}}{m_{l_j}}V^{cu\tilde{d}}_{RiAX}V^{cu\tilde{d}*}_{LjAX}\right] \tag{C10}$$

with $x_{AX}=(m_{u_A}/m_{\tilde{d}_X})^2$.

5. *W*-neutralinos

For *W*-neutralinos the amplitude in the unitary gauge ($\xi\to+\infty$) is

$$A_{Lij}^{N^0\text{-}W^\pm}=\sum_{A=1}^{5}-\frac{1}{32\pi^2}\frac{1}{m_W^2}\left[f_W(x_A)V^{cnW}_{RiA}V^{cnW*}_{RjA}+h_W(x_A)\frac{m_{\chi^0_A}}{m_{l_j}}V^{cnW}_{RiA}V^{cnW*}_{LjA}\right] \tag{C11}$$

with $x_A=(m_{\chi^0_A}/m_W)^2$ and the functions f_W, h_W given by

$$f_W(x)=\frac{10-43x+78x^2-49x^3+4x^4+18x^3\ln x}{6(1-x)^4},$$

$$h_W(x)=\frac{-4+15x-12x^2+x^3+6x^2\ln x}{(1-x)^3}. \tag{C12}$$

6. *Z*-charginos

For *Z*-charginos the amplitude in the unitary gauge ($\xi \to +\infty$) is

$$A_{Lij}^{C^{\pm}-Z^0} = \sum_{A=1}^{5} \frac{1}{32\pi^2} \frac{1}{m_Z^2} \left[f_Z(x_A) V_{RiA}^{ccZ} V_{RjA}^{ccZ*} + h_Z(x_A) \frac{m_{\chi_A^{\pm}}}{m_{l_j}} V_{RiA}^{ccZ} V_{LjA}^{ccZ*} \right] \tag{C13}$$

with $x_A = (m_{\chi_A^{\pm}}/m_Z)^2$ and the functions f_Z, h_Z given by

$$f_Z(x) = \frac{8 - 38x + 39x^2 - 14x^3 + 5x^4 - 18x^2 \ln x}{6(1-x)^4}, \qquad h_Z(x) = \frac{-4 + 3x + x^3 - 6x \ln x}{(1-x)^3}. \tag{C14}$$

[1] Super-Kamiokande Collaboration, Y. Fukuda *et al.*, Phys. Lett. B **433**, 9 (1998); **436**, 33 (1998); Phys. Rev. Lett. **81**, 1562 (1998).

[2] Chooz Collaboration, M. Apollonio *et al.*, Phys. Lett. B **420**, 397 (1998).

[3] B. Mukhopadhyaya and A. Raychaudhuri, Phys. Rev. D **42**, 3215 (1990); Kaon Physics Working Group Collaboration, A. Belyaev *et al.*, hep-ph/0107046; Eur. Phys. J. C **22**, 715 (2000).

[4] S.T. Petcov, Sov. J. Nucl. Phys. **25**, 340 (1977); T.P. Cheng and L.F. Li, Phys. Rev. D **16**, 1425 (1977); B.W. Lee and R.E. Shrock, *ibid.* **16**, 1444 (1977); J.D. Bjorken *et al.*, *ibid.* **16**, 1474 (1977); S.M. Bilenkii, S.T. Petcov, and B. Pontecorvo, Phys. Lett. **67B**, 309 (1977); S.M. Bilenkii and S.T. Petcov, Rev. Mod. Phys. **59**, 671 (1987); **61**, 169(E) (1989); A. Ilakovac and A. Pilaftsis, Nucl. Phys. **B437**, 491 (1995); J.G. Korner, A. Pilaftsis, and K. Schilcher, Phys. Lett. B **300**, 381 (1993).

[5] R. Barbieri and L.J. Hall, Phys. Lett. B **338**, 212 (1994); R. Barbieri *et al.*, Nucl. Phys. **B445**, 219 (1995); S. Dimopoulos and D. Sutter, *ibid.* **B452**, 496 (1995); Nima Arkani-Hamed, Hsin-Chia Cheng, and L.J. Hall, Phys. Rev. D **53**, 413 (1996); P. Ciafaloni, A. Romanino, and A. Strumia, Nucl. Phys. **B458**, 3 (1996); M.E. Gómez and H. Goldberg, Phys. Rev. D **53**, 5244 (1996); B. de Carlos, J.A. Casas, and J.M. Moreno, *ibid.* **53**, 6398 (1996); J. Hisano, T. Moroi, K. Tobe, and M. Yamaguchi, Phys. Lett. B **391**, 341 (1997); **397**, 357(E) (1997); S.F. King and M. Oliveira, Phys. Rev. D **60**, 035003 (1999).

[6] D.F. Carvalho, M.E. Gomez, and S. Khalil, J. High Energy Phys. **07**, 001 (2001).

[7] J. Hisano, T. Moroi, K. Tobe, and M. Yamaguchi, Phys. Rev. D **53**, 2442 (1996); M.E. Gómez, G.K. Leontaris, S. Lola, and J.D. Vergados, *ibid.* **59**, 116009 (1999); J. Ellis *et al.*, Eur. Phys. J. C **14**, 319 (2000); W. Buchmuller, D. Delepine, and F. Vissani, Phys. Lett. B **459**, 171 (1999); W. Buchmuller, D. Delepine, and L.T. Handoko, Nucl. Phys. **B576**, 445 (2000); Q. Shafi and Z. Tavartkiladze, Phys. Lett. B **473**, 145 (2000); J.L. Feng, Y. Nir, and Y. Shadmi, Phys. Rev. D **61**, 113005 (2000); J.A. Casas and A. Ibarra, Nucl. Phys. **B618**, 171 (2001); S. Lavignac, I. Masina, and C.A. Savoy, Phys. Lett. B **520**, 269 (2001); A. Kageyama, S. Kaneko, N. Shimoyama, and M. Tanimoto, *ibid.* **527**, 206 (2002).

[8] D.F. Carvalho, J.R. Ellis, M.E. Gomez, and S. Lola, Phys. Lett. B **515**, 323 (2001)

[9] M. Frank, Phys. Rev. D **62**, 015006 (2000).

[10] A. de Gouvea, S. Lola, and K. Tobe, Phys. Rev. D **63**, 035004 (2001).

[11] K. Cheung and O.C.W. Kong, Phys. Rev. D **64**, 095007 (2001).

[12] M. Hirsch and J.W.F. Valle, Nucl. Phys. **B557**, 60 (1999); M. Hirsch, J.C. Romão, and J.W. Valle, Phys. Lett. B **486**, 255 (2000).

[13] L.J. Hall, and M. Suzuki, Nucl. Phys. **B231**, 419 (1984).

[14] F. de Campos, M.A. García-Jareño, A.S. Joshipura, J. Rosiek, and J.W.F. Valle, Nucl. Phys. **B451**, 3 (1995); T. Banks, Y. Grossman, E. Nardi, and Y. Nir, Phys. Rev. D **52**, 5319 (1995); A.S. Joshipura and M. Nowakowski, *ibid.* **51**, 2421 (1995); H.P. Nilles and N. Polonsky, Nucl. Phys. **B484**, 33 (1997); B. de Carlos and P.L. White, Phys. Rev. D **55**, 4222 (1997); S. Roy and B. Mukhopadhyaya, *ibid.* **55**, 7020 (1997).

[15] J.C. Romão, M.A. Diaz, M. Hirsch, W. Porod, and J.W.F. Valle, Phys. Rev. D **61**, 071703 (2000); **62**, 113008 (2000).

[16] M.A. Díaz, J.C. Romão, and J.W.F. Valle, Nucl. Phys. **B524**, 23 (1998); for reviews see, e.g., J.W.F. Valle, ''Super-Gravity Unification with Bilinear *R*-Parity Violation,'' in Proceedings of 6th International Symposium on Particles, Strings and Cosmology (PASCOS 98), Boston, MA, 1998, edited by P. Nath, hep-ph/9808292; M.A. Díaz, talk given at International Europhysics Conference on High Energy Physics, Jerusalem, Israel, hep-ph/9712213.

[17] A. Masiero and J.W.F. Valle, Phys. Lett. B **251**, 273 (1990); J.C. Romão, C.A. Santos, and J.W.F. Valle, *ibid.* **288**, 311 (1992); J.C. Romão, A. Ioannissyan, and J.W.F. Valle, Phys. Rev. D **55**, 427 (1997); for a review, see J.C. Romão, ''Spontaneous Breaking of *R*-Parity,'' Proceedings of Beyond the Standard Model: From Theory to Experiment, Valencia, 1997, edited by I. Antoniadis, L.E. Ibanez, and J. W. F. Valle (World Scientific, Singapore, 1998), pp. 165–176, hep-ph/9712362.

[18] M.A. Diaz, J. Ferrandis, J.C. Romão, and J.W.F. Valle, Phys. Lett. B **453**, 263 (1999).

[19] M.A. Diaz, J. Ferrandis, J.C. Romão, and J.W.F. Valle, Nucl. Phys. **B590**, 3 (2000).

[20] For papers discussing *R*-parity violation phenomenology see, e.g., F. de Campos, O.J. Eboli, M.A. Garcia-Jareno, and J.W. Valle, Nucl. Phys. **B546**, 33 (1999); M. Nowakowski and A. Pilaftsis, *ibid.* **B461**, 19 (1996); L. Navarro, W. Porod, and J.W. Valle, Phys. Lett. B **459**, 615 (1999); M.A. Diaz, D.A. Restrepo, and J.W. Valle, Nucl. Phys. **B583**, 182 (2000); B. Allanach *et al.*, hep-ph/9906224; A. Faessler, S. Kovalenko,

and F. Simkovic, Phys. Rev. D **58**, 055004 (1998); S. Davidson, M. Losada, and N. Rius, Nucl. Phys. **B587**, 118 (2000); M. Bisset, O.C.W. Kong, C. Macesanu, and L.H. Orr, Phys. Rev. D **62**, 035001 (2000); M.A. Diaz, E. Torrente-Lujan, and J.W.F. Valle, Nucl. Phys. **B551**, 78 (1999).

[21] A. Akeroyd, M.A. Díaz, J. Ferrandis, M.A. Garcia-Jareño, and J.W.F. Valle, Nucl. Phys. **B529**, 3 (1998).

[22] A. Faessler, S. Kovalenko, and F. Simkovic, Phys. Rev. D **58**, 055004 (1998).

[23] A. Faessler, T.S. Kosmas, S. Kovalenko, and J.D. Vergados, Nucl. Phys. **B587**, 25 (2000).

[24] Particle Data Group, D.E. Groom *et al.*, Eur. Phys. J. C **15**, 1 (2000).

[25] L.M. Barkov *et al.*, Research Proposal to PSI, 1999, http://www.icepp.s.u-tokyo.ac.jp/meg.

[26] The homepage of the PRISM project: http://www-prism.kek.jp/; Y. Kuno, ''Lepton Flavor Violation Experiments at KEK/JAERI Joint Project of High Intensity Proton Machine,'' in Proceedings of Workshop of LOWNU/NOON 2000, Tokyo, 2000.

[27] H.E. Haber and G.L. Kane, Phys. Rep. **117**, 75 (1985); J.F. Gunion and H.E. Haber, Nucl. Phys. **B272**, 1 (1986); **B402**, 567(E) (1993).

[28] M.E. Gomez and K. Tamvakis, Phys. Rev. D **58**, 057701 (1998).

[29] R. Hempfling, Nucl. Phys. **B478**, 3 (1996).

[30] D.E. Kaplan and A.E. Nelson, J. High Energy Phys. **01**, 033 (2000).

[31] M. Hirsch, W. Porod, M.A. Díaz, J.W.F. Valle, and J.C. Romão, in Proceedings of the Corfu Summer Institute, Corfu 2001, hep-ph/0202149; M. Hirsch, W. Porod, M. A. Díaz, J. W. F. Valle and J. C. Romão (in preparation).

[32] M. Nowakowski and A. Pilaftsis, Nucl. Phys. **B461**, 19 (1996).

[33] J.R. Ellis, D.V. Nanopoulos, and K.A. Olive, Phys. Lett. B **508**, 65 (2001). and references therein.

[34] M. Drees and M.M. Nojiri, Phys. Rev. D **45**, 2482 (1992).

[35] For recent work on the topic see, for example, U. Chattopadhyay and P. Nath, Phys. Rev. D **53**, 1648 (1996); T. Moroi, *ibid.* **53**, 6565 (1996); M. Carena, M. Giudice, and C.E.M. Wagner, Phys. Lett. B **390**, 234 (1997); E. Gabrielli and U. Sarid, Phys. Rev. Lett. **79**, 4752 (1997); T. Ibrahim and P. Nath, Phys. Rev. D **61**, 095008 (2000); **62**, 015004 (2000); K.T. Mahanthappa and S. Oh, *ibid.* **62**, 015012 (2000); U. Chattopadhyay, D.K. Ghosh, and S. Roy, *ibid.* **62**, 115001 (2000).

[36] Muon g-2 Collaboration, H.N. Brown *et al.*, Phys. Rev. Lett. **86**, 2227 (2001).

[37] M. Knecht and A. Nyffeler, Phys. Rev. D **65**, 073034 (2002); I. Blokland, A. Czarnecki, and K. Melnikov, Phys. Rev. Lett. **88**, 071803 (2002); M. Knecht, A. Nyffeler, M. Perrottet, and E. De Rafael, *ibid.* **88**, 071802 (2002); M. Hayakawa and T. Kinoshita, hep-ph/0112102; J. Bijnens, E. Pallante, and J. Prades, Nucl. Phys. **B626**, 410 (2002).

[38] W. Porod, M. Hirsch, J. Romão, and J.W.F. Valle, Phys. Rev. D **63**, 115004 (2001).